PCCP
Physical Chemistry Chemical Physics

Accepted Manuscript

This article can be cited before page numbers have been issued, to do this please use: J. F. Sánchez M, M. D. Sanchez, R. D. Falcone and H. A. Ritacco, *Phys. Chem. Chem. Phys.*, 2021, DOI: 10.1039/D1CP05049D.

View Article Online
DOI: 10.1039/D1CP05049D

ARTICLE

Production of Pd Nanoparticles in Microemulsions. Effect of Reaction Rate on Particle Size.

Received 00th January 20xx,
Accepted 00th January 20xx

DOI: 10.1039/x0xx00000x

Jhon F. Sánchez M.[a], Miguel D. Sánchez[a], R. Dario Falcone[b] and Hernán A. Ritacco[*a]

In the synthesis of metallic nanoparticles in microemulsions, we hypothesized that particle size is controlled by the reaction rate not by microemulsion size. Thus, the changes observed on the particle sizes as reaction conditions, such as concentrations, temperature, type of surfactant used, etc., are varied should not be correlated directly to the modification of those conditions but indirectly to the changes they produce on the reaction rates.

In this work, the microemulsions were formulated with benzene and water as continuous and dispersed phases respectively, using n-Dodecyltrimethylammonium bromide (DTAB) and n-octanol as surfactant and cosurfactant. Using time-resolved UV-vis spectroscopy, we measured the reaction rates in the production of Palladium (Pd) nanoparticles inside microemulsions at different reactant concentrations and temperatures, keeping all the other parameters constant. The measured reaction rates were then correlated with the particle sizes measured by transmission electron microscopy (TEM).

We found that nanoparticle size increases linearly as the reaction rates increases, independently of the actual reactant concentrations or temperature. We proposed a simple model for the observed kinetics where the reaction rate is controlled mainly by the diffusion of the reducing agent. With this model, we predicted that particle size should depend indirectly, via the reaction kinetics, on the micelle radius, the water volume and the total microemulsion volume. Some of these predictions were indeed observed and reported in the literature.

Introduction

Microemulsions[1] are thermodynamically stable dispersions of immiscible liquids, in general water and oil, that are stabilized by some chemical agent in general, a surfactant[2]. Surfactants are amphiphilic molecules containing different chemical groups on their structures, some of them with affinity for one of the liquids in the dispersion, and some others with affinity for the other liquid. Because of this, they place themselves spontaneously on the interface between the liquids, exposing their chemical groups in the direction of the liquid for which they have affinities, reducing the surface tension, and stabilizing the dispersion. The synthesis of nanoparticles in microemulsions was proposed in the 1980s as a method for obtaining monodisperse particles with perfectly controlled sizes. The term "reverse micelles" or "water-in-oil" (W/O) microemulsions refers to droplets of water dispersed in a continuous phase of oil, in opposition to direct or oil-in-water (O/W) microemulsion that refers to droplets of oil dispersed in water[1–3]. In this sense, reverse micelles are organized systems coexisting in water-in-oil (W/O) microemulsions and both definitions (reverse micelles and microemulsions) are normally used as synonyms but are not equal. The concept of the microemulsion applies to a liquid solution composed of water, oil, and an amphiphile (surfactant and cosurfactant) forming a single, optically isotropic and thermodynamically stable phase[4]. Thus, a microemulsion shows a certain degree of the intermolecular arrangement but without a well-defined stoichiometric composition. On the other hand, reverse micelles solutions are systems with a strong molecular organization[5].

Since its formulation[6], the synthesis of nanoparticles via microemulsions[7] has become a widely used technique[8] for the preparation of a diversity of nanoparticles[9,10]. There are several reviews on the subject[8,11–16]. Among the particles that can be produced by this method, a great variety of precursors have been used to obtain metallic nanoparticles including nickel[17], gold[18,19], silver[20], platinum[21], and palladium[22]. We are particularly interested in the synthesis of Pd nanoparticles due to their physicochemical properties and the possibility of using

[a] Instituto de Física del Sur (IFISUR), Departamento de Física, Universidad Nacional del Sur (UNS), CONICET, Av. L. N. Alem 1253, B8000CPB - Bahía Blanca, Argentina..
[b] Departamento de Química, Universidad Nacional de Río Cuarto (UNRC). Instituto para el Desarrollo Agroindustrial y de la Salud (IDAS), CONICET–UNRC, Agencia Postal No. 3, X5804BYA Río Cuarto, Argentina.
(*) Corresponding author: hernan.ritacco@uns.edu.ar

Electronic Supplementary Information (ESI) available: ESI includes additional and supplementary experimental results. Fig. ESI-1: DLS results; Fig.ESI-2: UV-vis spectra at different concentrations of reactants in water; Fig. ESI-3: idem ESI-2 in the microemulsions; Fig. ESI-4: calibration curve for reactant concentration; Fig. ESI-5: UV-vis results as a function of concentration and time; Fig. ESI-6: kinetic of reaction at different concentrations; Fig. ESI-7: microemulsion size as a function of temperature (DLS); Fig. ESI-8: Kinetic of reaction as a function of temperature; Fig. ESI-9: TEM results; Fig. ESI-10: TEM results for particles obtained in water and in microemulsions. See DOI: 10.1039/x0xx00000x

DOI: 10.1039/D1CP05049D

them for catalytic purposes[23–25]. These properties are strongly related to the size and structure of the obtained nanoparticles[26]; hence, studies on growth control and size distribution have received a great deal of attention in recent years[27–31].

Although microemulsions as nanoreactors have been used successfully to produce several nanostructures of different sizes and shapes[16,32], the role played by microemulsions in tailoring those structures is still unresolved. In the early days of the method, it was considered that the size of the particles obtained depended mainly on the size of the droplets in the microemulsion, the water pool acting as a template in defining the final size and the structure of the nanoparticle. However, it is not always possible to find a direct correlation between the size of the aqueous core of the droplets and the size of the synthesized nanoparticle[15], although in some cases it is[33]. The control of size is a complex phenomenon, which involves mechanisms of chemical kinetics and mass transfer between the micelles[34]. These mechanisms and, therefore, the final size of the nanoparticles would be affected by other control variables, such as the concentration of the reagents in the drops[35], the amount of water[29], the flexibility or rigidity of the surfactant film[36], the capability of the surfactants/co-surfactants in protecting the particles against aggregation and coarsening, and even the autocatalytic growth processes[37]. Additionally, an important number of published works have experimentally and theoretically studied the effects of micellar exchange concerning the kinetics of the formation and growth of nanoparticles[38–41]. However, the literature on the experimental base is still scarce and the effect of intermicellar dynamics and control variables on the size of the particles is far from being understood, mainly because of the huge number of parameters that influences the synthesis results[8,27,40,42,43].

In this article, we study systematically the reaction kinetics in the production of metallic nanoparticles of Palladium (Pd) in microemulsions using UV-vis spectroscopy. The palladium salt precursor used, $PdCl_4^{-2}$, has an adsorption peak at 425 nm, which allows us to follow the reaction kinetics without interferences of particle growth by coalescence and coarsening. This is possible because Pd has no localized surface plasmon resonances (LSPR) in the UV-vis at wavelength > 200 nm, for spherical particles with sizes below 30 nm[44]. We will see that in this work the particles sizes are all below 9 nm, which facilitates the study of the reaction kinetics by UV-vis spectroscopy and that is the reason why we have chosen this model system to test our hypothesis.

The microemulsions were formulated with benzene and water as continuous and dispersed phases respectively, using n-Dodecyltrimethylammonium bromide (DTAB) and n-octanol as surfactant and cosurfactant. We focused our attention on the relationship between the initial reaction rates and the final particle size. We changed the reaction rates by changing the reactant concentrations and temperature. We found a linear correlation between the initial reaction rates and the final particle size independently of the actual concentrations or temperature. In other words, for this particular system, the nanoparticle size depends indirectly on reactant concentrations and temperature via the reaction rate. A simple model is proposed to rationalize our findings.

Materials and Methods

Chemicals, main reaction and microemulsion preparations.

Palladium(II) chloride ($PdCl_2$), sodium borohydride ($NaBH_4$), n-dodecyltrimethylammonium bromide (DTAB), hydrochloric acid (HCl), n-octanol ($C_8H_{18}O$), and benzene (C_6H_6) were used in the formulation of the microemulsions. All reagents were of analytical grade, and they were used directly without further purification. The water used to prepare the solutions was from Mili-Q® ultrapure water purification system.

We prepared aqueous solutions of Pd(II) ions (~ 10^{-3} M) that were obtained by dissolving $PdCl_2$(s) in HCl/H_2O (6 mM). We used $NaBH_4$ solutions in water at different concentrations ranging from 30 to 120 mM as a reducing agent. Two identical solutions were prepared with microemulsions containing Pd(II) and $NaBH_4$, respectively. Precisely measured volumes (~1 cm^3) of the precursor solutions were injected into 5 ml of a benzene/DTAB/n-octanol mixture, [DTAB]=0.1M, [n-octanol]= 0.7 M. The molar ratio of water to DTAB, defined as W_0 = [water]/[surfactant] in each microemulsion was W_0=15.

The nanoparticles were synthesized by rapidly mixing equal volumes (1 cm^3) of the microemulsions, with one volume containing palladium ions and the other one containing adequate amounts of $NaBH_4$ as a reducing agent. The reaction kinetics was measured by following the reduction of the absorbance peak at a wavelength of 340 nm by Ultraviolet-visible spectroscopy. This peak is the 425 nm peak mentioned in the introduction and characteristic of the complex $[PdCl_4]^{-2}$, but shifted to a lower wavelength due to the presence of the microemulsions.

The mechanism of the reaction should be considered when discussing the kinetics of particle production in the following sections. In particular, we want to stress that the chemical reaction involved in the production of Pd particles consists of two reactions: the hydrolysis of the reducing agent that ends in a release of gaseous hydrogen[45],

$$NaBH_4 + 2H_2O \rightarrow NaBO_2 + 4H_2 \quad (1)$$

and the reduction of palladium(II) ions (in HCl (aq)) by gaseous hydrogen[46]

$$[PdCl_4]^{-2} + H_2 \rightleftharpoons Pd^0\downarrow + 4Cl^- + 2H^+ \quad (2)$$

Due to the fast hydrolysis and the production of H_2, all experiments of the reaction kinetics were performed with $NaBH_4$ solutions freshly prepared: no more than 10 minutes elapsed between the preparation of the microemulsion with $NaBH_4$ and its use in the reaction kinetics experiments. It is relevant to mention here that after about 2 hs, the $NaBH_4$ aqueous solutions lost their capacity of acting as a reduction

View Article Online
DOI: 10.1039/D1CP05049D

agent. This is a clear indication of the production of H_2 in hydrolysis.

Characterization Methods

The size of the microemulsion was determined with the dynamic light scattering (DLS) technique by using a multi-angle Malvern auto-sizer 4700 system equipped with an OBIS laser (λ=514nm, 20 mW).

As previously mentioned, the reaction kinetics was followed by UV-vis spectrometry after mixing two identical microemulsions: one containing the Pd ions and the other one containing the reduction agent. All the measurements were conducted in an Ocean Optics USB2000 miniature spectrophotometer with a measuring wavelength range of 200-800 nm. A quartz cuvette with an optical path of 1 cm was used.

The determination of particle size distribution was performed manually from the digital analysis of the transmission electron microscopy (TEM) images using fresh samples prepared in situ. A few drops of the microemulsion containing the palladium solid material were taken and deposited directly on the carbon-coated copper grids used for TEM. We used a JEOL-100CX II microscope operating at 100 kV for the majority of TEM measurements. Additionally, we used a FEI Talos F200X™ (Thermo Scientific™) Scanning/Transmission Electron Microscope equipped with a Super-X EDS (Energy Dispersive Spectrum) composed of 4 windowless detectors. The equipment was operated at 200 kV in high-resolution mode (HRTEM). Scanning/Transmission Electron Microscope (STEM) images were obtained using a High-Angle Annular Dark-Field (HAADF) detector. For each sample, the average size and standard deviation were determined from a minimum of 250 particles from different parts of the grid.

Results

In what follows we will first present results of the reaction rates as a function of precursor and reducing agent concentrations. Then we will show results about reaction rates as a function of temperature. Finally, we will present results of particles sizes showing that they correlate with reaction rates regardless of concentrations or temperature.

Effect of precursors concentration in microemulsion sizes.

Figure ESI-1 shows the hydrodynamic diameter distribution of microemulsion droplets as measured by Dynamic Light Scattering. We performed the measurements in microemulsions containing different amounts of $PdCl_2$ and also $NaBH_4$ to confirm that no changes occur in the microemulsion droplet size. The apparent hydrodynamic diameter of the micelles was about 10 nm, independently of the chemical concentrations. We also measured by DLS the droplet size after the reaction. No appreciable variations in the average diameter of the micelles were observed after the reaction was completed.

Likewise, no appreciable variations in time were observed for the size distribution of the individual microemulsions containing the reagents. The measurements were made every 24 h during five consecutive days.

To probe our idea about the effect of the reaction kinetics on nanoparticle size, the microemulsion formulation was kept constant in all experiments. In this sense, we choose W_0=15 due to the microemulsions varying the precursor concentrations produce clear and stable dispersions for a long time.

Reaction kinetics of Pd nanoparticles formation.

As previously mentioned, the reaction kinetics in the formation of Pd nanoparticles was followed by UV-vis spectrophotometry. In the typical spectra shown in Figure 1a, two absorption peaks were identified at wavelengths 280 nm and 340 nm. Due to the medium conditions (pH=2.5), these peaks have been assigned to the UV-vis peaks that are characteristic of the ions $PdCl_4^{-2}$ [47]. The same peaks appear in aqueous solutions of $PdCl_2$ in the presence of HCl at pH = 2.5 but shifted to 325 and 425 nm, respectively (see Figure ESI-2). The shift is a consequence of the confined environment of the microemulsions[48]. Because the observed transition moves to shorter wavelengths (higher energies), it is probable that the negatively charged complex $PdCl_4^{-2}$ is stabilized by the oppositely charged interface covered with cationic ions of DTAB. We have chosen following the kinetics using only the peak at 340 nm avoiding the possible interference of benzene (UV cutoff 280 nm) and, if present, Pd surface plasmon resonance[44]. It is worth mentioning that the position of the peak at 340 nm does not change as the concentration of the palladium precursor is changed in the microemulsion (see Figure ESI-3), assuring that the measured kinetics is not affected by a spurious movement of the position of the peak. Additionally, it was found that the microemulsions containing the $NaBH_4$ as a reducing agent do not absorb electromagnetic radiation in the range of 275 to 580 nm. The progress of the reaction is shown in Figure 1b, where the absorbance was transformed in Pd^{2+} ions concentration by a calibration curve (shown in Figures ESI-4). In all cases, a decrease in the UV-vis signal was observed up to a stable point associated with the end of the reaction. Given the amounts of the reducing agent, it can be assumed that the conversion of Pd(II) ions is close to 100% at all the concentrations explored.

To determine the rate law of the reduction reaction, experiments were performed under different conditions of concentration of the reagents.

From the curves like that the one shown in Figure 1b (and Figures ESI-5 and ESI-6), we obtained from the slopes the initial rates of the reactions, $v_0 = -\left.\frac{d[Pd^{2+}]}{dt}\right|_{t=0}$ as a function of the initial concentration of the reduction agent, $[NaBH_4]_0$, and for different concentrations of the precursor, $[PdCl_2]$. The results are presented in Figure 2.

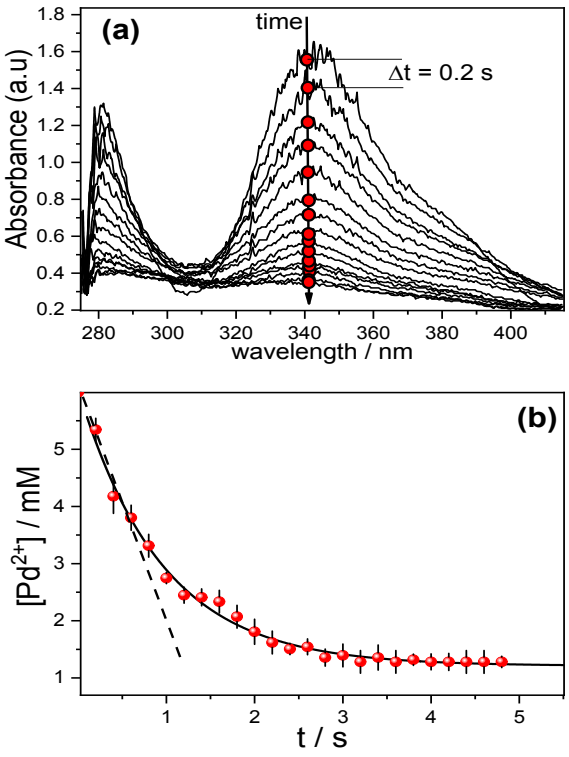

Figure 1: (a) UV-vis spectra measured at time intervals of 0.2 s during the reaction in the microemulsion. The peak at 340 nm is followed to determine the rate of reaction plotted in (b). The results correspond to the reaction with initial concentrations of $[PdCl2]_0$= 6 mM; $[NaBH_4]_0$= 90 mM; W_0=15.

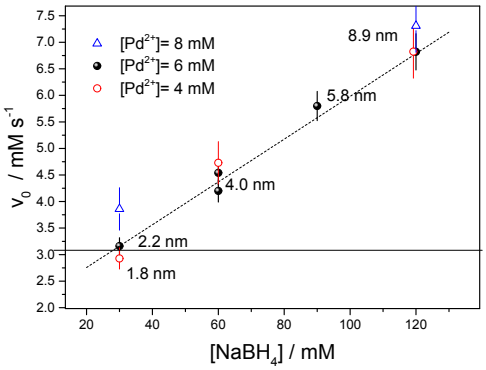

Figure 2: Initial reaction rate as a function of the concentration of the reduction agent for different concentrations of the Palladium salt. The mean diameter of the nanoparticles obtained after the reaction is inserted in the figure.

It can be observed that an increase in the reducing agent concentration leads to an increase in the reaction rate for the three concentrations of palladium studied, $[Pd^{2+}]$ = 8, 6 and 4 mM, being the reaction rate increment linear with the concentration of the reducing agent and with the same slope for the three concentrations of palladium. The reaction rates seem to be independent of the palladium concentration, within the errors and for 4<= $[Pd^{2+}]$<= 8. This is also clearly seen in Figure 3, where we present results of the initial reaction rates as a function of palladium concentration keeping the concentration of the reducing agent constant. The reaction rate does not change when the precursor, the palladium salt, concentrations are changed at a constant concentration of $NaBH_4$.

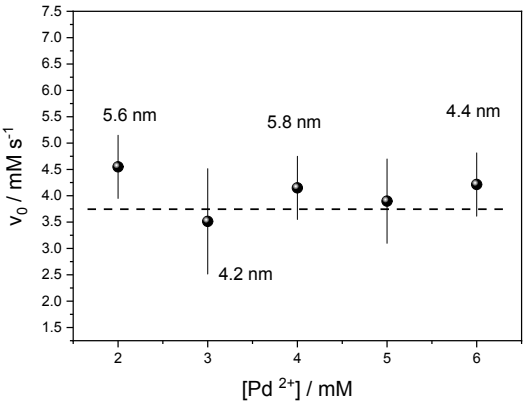

Figure 3 : Initial reaction rate as a function of the precursor concentration, PdCl2. The initial concentration of the reducing agent, $NaBH_4$, is fixed at 60 mM. The mean diameter of the obtained metallic Palladium nanoparticles is inserted on the figure.

Particle size, size distribution and morphology.

Once the equilibrium condition (constant absorbance value, see Figure 1b) was reached, we collected samples of each microemulsion containing the synthesized palladium nanoparticles. The samples were analysed by TEM to characterize them and to determine their size. Figure 4 shows images of the nanoparticles that were obtained for initial concentrations of $[NaBH_4]$ = 60 mM and $[Pd^{2+}]$ = 6 mM. The particles are quite monodisperse having an average diameter of 4.4 nm, which was confirmed by dark-field TEM micrographs. The particles were globular. The morphology is typical of palladium metal particles with face-centred cubic (fcc) symmetry. In the images of Figure 4, the lattice fringes of the particles that would be related to a crystalline structure were observed. The interplanar distance of 2.24 Å would correspond to the planes (111) of the face-centred cubic (fcc) structure of the metallic palladium.

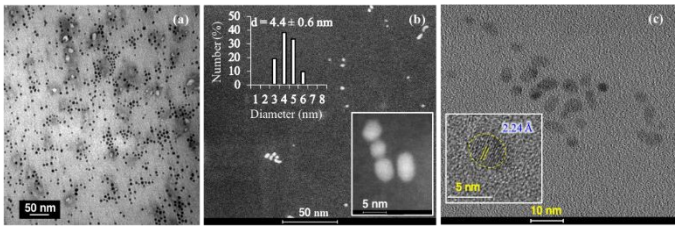

Figure 4: Analysis of the nanoparticles by high-resolution transmission electron microscopy (HR-TEM). (a) TEM micrograph of nanoparticles obtained with $[NaBH_4]$ = 60 mM and $[Pd^{2+}]$ = 6 mM. (b) Analysis using dark-field TEM and determination of size. (c) HR-TEM image. A typical Pd nanoparticle is shown.

Figure 5 shows representative images and the size distribution of the palladium nanoparticles that were synthesized in microemulsion at different reagents concentrations. From the results, it can be seen that the average particle size increases as

the amount of the reducing agent increases relative to palladium. The apparent average diameter of the synthesized nanoparticles varies between 2 and 9 nm, with a standard deviation (σ) that increases as the concentration of $NaBH_4$ increases.

All the measured sizes at the different reaction conditions were also indicated in the previous Figures 2 and 3. Note that, in all cases, the average diameter of the nanoparticles is less than the apparent hydrodynamic diameter of the microemulsion (~10 nm), as it was measured by Dynamic Light Scattering.

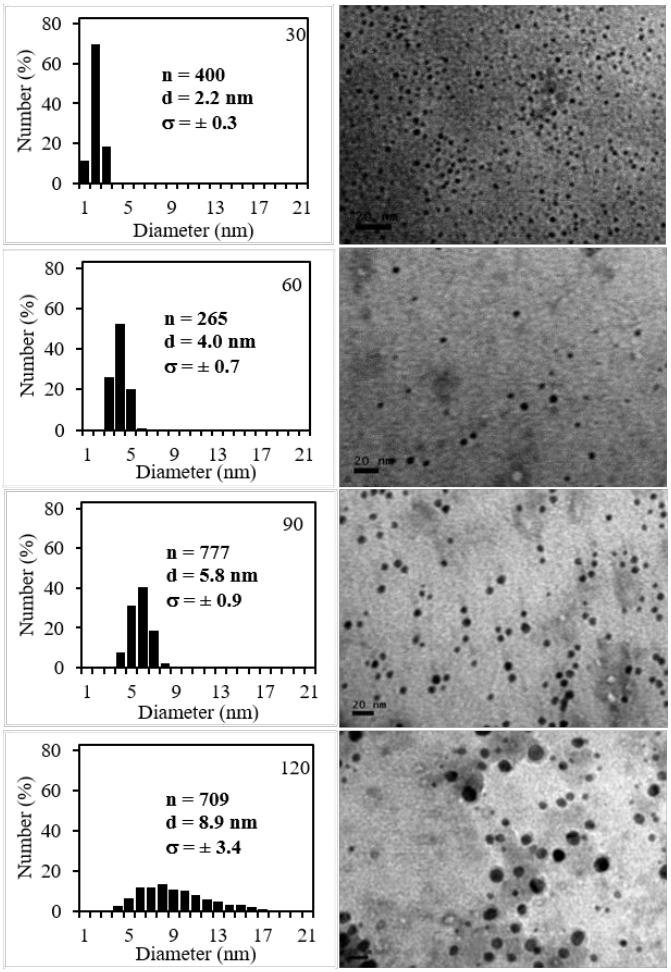

Figure 5: TEM micrographs and size distribution of the Pd nanoparticles obtained in microemulsion. Conditions from top to bottom, [$NaBH_4$] = 30, 60, 90 and 120 mM. In all cases [Pd^{2+}]=6 mM. Temperature = 25 °C. Scale: 20 nm. W_0=15.

Effect of Temperature on the Reaction Rates.

We measured first the dependence of the microemulsion hydrodynamic radius (r) on temperature, r(T). Figure ESI-7 shows the micelle diameter (2r) as measured by dynamic light scattering (hydrodynamic diameter) as a function of temperature for microemulsions containing only water, water + Pd salt at different concentrations, and water + $NaBH_4$ also at several concentrations, all prepared at the same molar ratio of water to DTAB (W_0=15). The size does not depend on reactant concentrations; it only depends on temperature. The micelle radius varies following a power law, $2r \sim (T-273.15)^{-0.18}$.

In Figure 6, we present results on the reaction rate as a function of temperature represented as the logarithm of the reaction rate vs the inverse of the absolute temperature. We observe an Arrhenius-like behaviour, $\ln(v_0) \sim -\frac{E_a}{RT}$, with E_a = 107 kJ/mol (=25.5 Kcal/mol), which is a physically reasonable value assuming that the reaction is limited by gas diffusion in the presence of the microemulsion interfaces covered with surfactants[50,51].

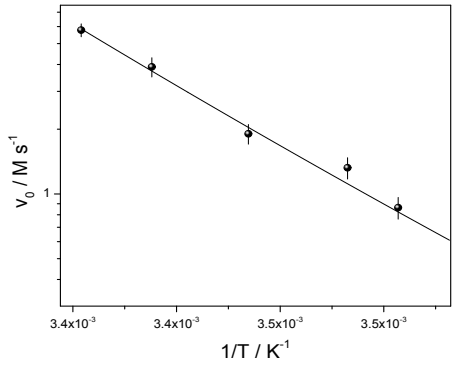

Figure 6: initial reaction rate as a function of the inverse of temperature. The line is a fitting with an Arrhenius- like function.

Effect of reaction rate on particle size.

As it was mentioned in the Introduction, our hypothesis of departure was that the particle size depends directly on the reaction rate (and indirectly on concentration, temperature, water-surfactant ratios, etc.). In Figure 7, we plotted the particle size measured by TEM microscopy as a function of the initial reaction rate, independently of the actual palladium precursor and reducing agent concentrations. A quite clear tendency can be observed: the lower the reaction rates, the smaller the particle size and particle size polydispersity (Figure 5). Let us remark here that the size is correlated with the reaction rate and not with the actual reactant concentration (or temperature), we can get the same initial reaction rates for different relations of Pd salt and $NaBH_4$ concentrations (or different temperatures).

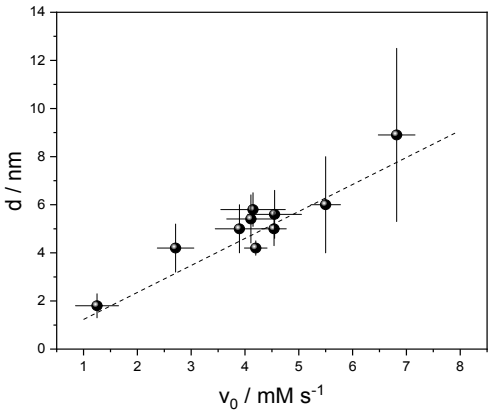

Figure 7: Particle size as a function of initial reaction rate. The line corresponds to a linear fitting: d(nm)~ v_0 *(mM/s)*.

In this Figure 7, each point at a given measured value of the reaction rate includes experiments performed at different concentrations of precursor, reducing agents, and temperature given a similar (±5%) initial reaction rate, v_0. Figure 7 shows that the particle diameter is approximately linear with the initial reaction rate, $d \sim v_0$.

Discussion

On an empirical basis, the initial reduction rate of the Pd(II) ions can be written as:

$$v_0 = k_{obs} \cdot [Pd^{2+}]_0^n \cdot [NaBH_4]_0^m \quad (3)$$

where v_0 is the initial reaction rate, k_{obs} is the observed reaction rate constant, $[Pd^{2+}]_0$ and $[NaBH_4]_0$ are the initial concentrations of the reactants, *n* and *m* are the reaction orders for the precursor and the reducing agent, respectively.

From the above results, and for $[Pd^{2+}] \geq 4$ mM, we found *n=0* and *m=1*. Thus, the reaction is independent of the palladium concentration and first order in the reducing agent (and globally). Under these conditions and from the slope of Figure 2 (considering all the performed experiments), the rate constant gives, k_{obs} = (0.040±0.002) s^{-1} (note that if hydrogen concentration, $[H_2]$ had been used instead of $[NaBH_4]$ in Figure 2, and considering the stoichiometry of the hydrolysis -see material section-, the kinetic constant would have given $k_{obs}/4$= 0.01s^{-1}).

To propose a possible reaction mechanism, let us stress some facts. The experimental observation that the reaction rate is first-order for the reducing agent and zero-order for the Pd salt could indicate that the reaction is controlled by the diffusion/transport mechanisms of the reduction agent, i.e. H_2. Because the ionic species, $PdCl_4^{-2}$, involved in the reaction could hardly be transferred through the oil phase[52], let us assume then that they remain in the water pool of the microemulsion. Thus, the unique way of transferring $PdCl_4^{-2}$ from one water pool to another is by collision and fusion of the micelles[53–58]. The situation for H_2 molecules is quite different; the solubility of H_2 is four times larger in benzene than in water. We already mentioned that the reducing properties of the microemulsion containing $NaBH_4$ disappear after 2 hs, which seems to indicate the transfer of H_2 out of the water pool of the microemulsion. Thus, the evidence indicates that H_2 can diffuse from one water pool to another through the continuous phase (oil). Based on this evidence we propose the reaction mechanism schematized in Figure 8, in which the Pd particles can be produced by two possible paths.

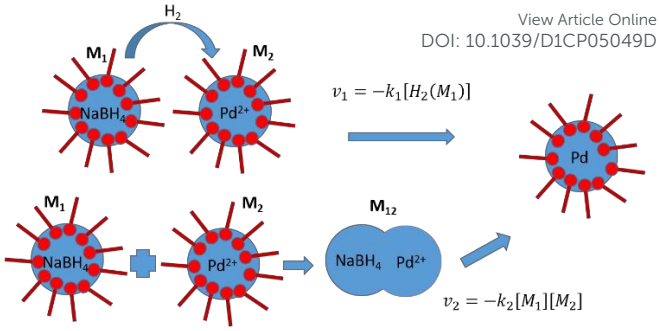

Figure 8: Scheme for the two possible paths for the reaction in the production of Pd nanoparticles.

One of them involves the diffusion of H_2 molecules from the micelles where they are produced through the continuous phase and then into a micelle containing the Pd precursor. The other reaction path considers the collision of two micelles, one containing the precursor and the other the reduction agent. If now we assume that the constants rates for the production of H_2 by hydrolysis and the reaction of H_2 with the palladium precursor are faster than the processes aforementioned and schematized in Figure 8, we can express the rate of production of Pd metallic particles considering only the two slower processes,

$$H_2(M_1) \rightarrow H_2(M_2);\ v_1 = -k_1[M_1] \quad (4)$$

Where $H_2(M_1)$ represents the hydrogen in microemulsion 1 (M_1, with reduction agent), and $H_2(M_2)$ the hydrogen transferred inside the microemulsion 2 (M_2, with Pd precursor), as represented in Figure 8. Similarly, for the second possible path,

$$M_1 + M_2 \rightarrow M_{12} \rightarrow 2\ Pd^{(0)}\ (M_1, M_2);\ v_2 = -k_2[M_1][M_2] \quad (5)$$

Thus, the rate of production of Pd metallic should be the sum of the two paths,

$$v = \frac{d[Pd^{(0)}]}{dt} = k_1[M_1] + k_2[M_1][M_2] = (k_1 + k_2[M_2])[M_1] \quad (6)$$

The initial concentration of the reduction agent, $[NaBH_4]_0$, and precursor, $[PdCl_4^{-2}]_0$, are proportional to $[M_1]$ and $[M_2]$ respectively thus, in the previous expression, we can replace one for the other. Recall that k_1 is related to H_2 diffusion, the coefficient diffusion of H_2 in benzene is ~10^{-9} m^2 s^{-1}; k_2 is related to micelles diffusion (and fusion), the diffusion coefficient of the micelles measured by DLS is ~10^{-11} m^2 s^{-1}. Thus, it is reasonable to consider that $k_2[M_2] \ll k_1$, and then,

$$v \sim k_1[M_1] \propto k_1[H_2(M_1)]_0 \quad (7)$$

View Article Online
DOI: 10.1039/D1CP05049D

Note that the reaction rate law is of pseudo-first-order in H_2 and zero-order in Pd precursor, as it was observed experimentally.

The Kinetic constant, k_1

The kinetic constant k_1 corresponds to the diffusion of H_2 from their microemulsion M_1, into the microemulsion containing the Pd precursor, M_2; it could be expressed in terms of an effective diffusion coefficient,

$$v_1 \sim J\,A = -D_{eff}A\frac{d[H_2]}{dx} \sim D_{eff}A\frac{\Delta[H_2]}{\Delta x} = D_{eff}\frac{A_m(N/2)}{l}[H_2] \quad (8)$$

where we have used the one-dimensional Fick's law to write the reactant diffusion flux, *J* (moles per unit of area and time); A is the total area of the micelles per unit volume (A~ (N/2). A_m; $A_m=4\pi r^2$ being r the micelle radius and N the number of microemulsions per total volume) and *l* the diffusion distance. Thus, the kinetic constant reads,

$$k_1 = D_{eff}\frac{A_m(N/2)}{l} \quad (9)$$

Equation 9 predicts that the kinetic constant k_1 depends on the size of the microemulsion via the area, A_m, the concentration of microemulsion, N, and the distance between them, *l*. Note that N is the number of microemulsion droplets per unit volume, $\approx \frac{V_w}{\left(4/3\pi r^3\right)}\frac{1}{V_T}$, being V_w the volume of water added, r the radius of the microemulsion, and V_T the total volume of the microemulsion. We could estimate the distance between micelles from the mean free path, $\sim\frac{1}{N\pi r^2}$, then the kinetic constant should scale as,

$$k_1 \sim D_{eff}\left(\frac{V_w}{V_T}\right)^2\frac{1}{r^2} \quad (10)$$

Note that equation 10 predicts that reaction rates will depend on water and total volume in the microemulsion. Despite the oversimplification and naivety of the model that leads to eq. 10, the effect of the content of water in the microemulsion and total volume, V_w and V_T, on the size of particles obtained by reaction in microemulsions was recently observed and reported [29]. Additionally, note that equation 6 predicts that the reaction rate depends on the concentration of microemulsion droplets

Comments on nucleation, growth and size dependence.

However, the discussion that follows is speculative and should be verified experimentally, let us discuss the process of nucleation and growth of the nanoparticles in microemulsions in the context of nucleation and growth theories in solution[59,60]. One of the most well-known ideas from nucleogenesis theories is the explanation of the production of monodisperse colloids[61]. The classical nucleation theory predicts that the rate of nuclei production, dN_u/dt, where N_u is the number of nuclei produced and t the time, yields[60]

$$\frac{dN_u}{dt} \sim e^{-\frac{\gamma^3 V^2}{(k_B T)^3 [ln(R)]^2}} \quad (11)$$

being γ the interfacial tension, V the particle volume, R the supersaturation ratio, $R=S_{ss}/S_0$, here S_{ss} would be the actual concentration of atomic Pd, and S_0 the equilibrium solubility limit of atomic Pd ($S_{ss}>S_0$). This equation indicates that the rate at which the particle nuclei is produced increases with the supersaturation ratio, being this the controlling parameter. In our case, this depends on the reaction rate; if it is slow, the production of a few nuclei reduces appreciably the Pd concentration and relieves the supersaturation, resulting in a reduction of the rate of nucleation (Eq. 8). Consequently, by reducing the reaction rate, the period in which nucleation can occur is reduced in such a way that monodispersed particles result from the uniform growth of the existing nuclei. In this regime, a balance between the rate of production of metallic Pd and the removal by diffusion onto the nuclei is attained. These monodisperse particles would be protected by the microemulsion, which slows down the coalescence dynamics among them.

On the contrary, when the rate of reaction is high, the rate of production of Pd metallic atoms during the chemical reaction becomes so rapid that the supersaturation remains, and the nuclei are produced continuously while the existing nuclei grow. In this regime, the size of any given particle will depend upon when it was created. As a consequence, the particle size distribution broadens, becoming polydisperse (see Figure 5). This explains the increased polydispersity, but to explain the increase in the particle size as the reaction rate increases, it is necessary to include in the discussion the dynamics of particle coalescence and Ostwald ripening (coarsening). The rapid production of nuclei simultaneously with the growth of the existing ones in conjunction with the processes of collision, fusion and intermicellar exchange of material should permit the coalescence of Pd particles and their growth by coarsening, a process that should not be possible if the production of Pd metallic atoms is slow.

Summary and Conclusions

In this article, we presented a systematic study of the reaction kinetics of $PdCl_2$ with $NaBH_4$ for the production of metallic Pd nanoparticles in microemulsions. Our work was based on the assumption that the reaction rate is the main factor controlling the final particle size. We found that the final particle size is well correlated with the initial reaction rate, and not directly correlated with parameters such as reactant concentrations or temperature. Those parameters effectively modify the final particle size, but indirectly by changing the reaction rates.

To explain the reaction kinetics in our systems, we departed from the commonly accepted view of considering the process of mixing the reactants by intermicellar exchange [13,14,54,56,62]:

once the microemulsions containing the precursor and the reducing agent are mixed, the droplets collide, fuse, interchange the material and break apart again but not being this process the unique way of producing the mixing of the reactants. In our system, we considered the possibility that the reducing agent diffuses out of the water pool into the continuous phase. This was based on three experimental facts: first, $NaBH_4$ in contact with water hydrolyses to produce H_2; second, H_2 is four times more soluble in benzene, the continuous phase, than in water; third, the capability of acting as a reducing agent of the $NaBH_4$ disappears after 2 hs, which indicates that the H_2 can effectively go out the water pools of the microemulsion. Additionally, the reaction kinetics was experimentally found to be first order in $NaBH_4$ and zero-order in the precursor of palladium. This last experimental fact leads us to propose a simple reaction mechanism that allows explaining some of the experimental findings. We also presented a quite naïve diffusional model to express the kinetic constant that predicts how the reaction rates depend on the micelle size, the water volume, the microemulsion total volume and the concentration of microemulsions droplets. However, the specific dependence of the kinetic constant with r, V_w and V_T in equation 10 is probably incorrect, some of these predictions about their influence in particle size were indeed observed in the production of nanoparticles in microemulsions [22,29,63,64]. In this respect, we will work in the near future on how the reaction kinetics depends on the micelle radii, the water content and the total microemulsion volume. The influence of the interfacial elasticity and the use of different oils as the continuous phase, all parameters suspected of modifying the effective diffusion coefficients, will be studied as well.

Conflicts of interest

There are no conflicts to declare.

Acknowledgements

This work was supported, in part, by Universidad Nacional del Sur (UNS, Argentina) under grants PGI-UNS 24/F080 and 24/F082; by Agencia Nacional de Promoción Científica y Tecnológica (ANPCyT, Argentina) under grant PICT-2016-0787, and by Consejo Nacional de Investigaciones Científicas y Técnicas (CONICET, Argentina) under grant PIP-GI 2019 Nro 11220200101754CO.
The authors would like to thank Dr. Alberto Caneiro from Y-TEC (YPF Tecnología, Argentina) for his contribution to the HRTEM characterizations.

Notes and references

1 D. Langevin, Microemulsions, *Acc. Chem. Res.*, 1988, **21**, 255–260.
2 D. Langevin, Micelles and Microemulsions, *Annu. Rev. Phys. Chem.*, 1992, **43**, 341–369.
3 D. Langevin, Microemulsions - interfacial aspects, *Adv. Colloid Interface Sci.*, 1991, **34**, 583–595.
4 I. Danielsson and B. Lindman, The definition of microemulsion, *Colloids and Surfaces*, 1981, **3**, 391–392.
5 N. M. Correa, J. J. Silber, R. E. Riter and N. E. Levinger, Nonaqueous Polar Solvents in Reverse Micelle Systems, *Chem. Rev.*, 2012, **112**, 4569–4602.
6 M. Boutonnet, J. Kizling, P. Stenius and G. Maire, The preparation of monodisperse colloidal metal particles from microemulsions, *Colloids and Surfaces*, 1982, **5**, 209–225.
7 B. K. Paul and S. P. Moulik, Microemulsions: an Overview, *J. Dispers. Sci. Technol.*, 1997, **18**, 301–367.
8 S. a Tovstun and V. F. Razumov, Preparation of nanoparticles in reverse microemulsions, *Russ. Chem. Rev.*, 2011, **80**, 953–969.
9 J. A. Gutierrez, R. D. Falcone, M. A. Lopez-Quintela, D. Buceta, J. J. Silber and N. M. Correa, On the investigation of the droplet-droplet interactions of sodium 1,4-bis(2-ethylhexyl) sulfosuccinate reverse micelles upon changing the external solvent composition and their impact on gold nanoparticle synthesis, *Eur. J. Inorg. Chem.*, 2014, 2095–2102.
10 J. A. Gutierrez, M. Alejandra Luna, N. Mariano Correa, J. J. Silber and R. Darío Falcone, The impact of the polar core size and external organic media composition on micelle–micelle interactions: the effect on gold nanoparticle synthesis, *New J. Chem.*, 2015, **39**, 8887–8895.
11 M. P. Pileni, Control of the size and shape of inorganic nanocrystals at various scales from nano to macrodomains, *J. Phys. Chem. C*, 2007, **111**, 9019–9038.
12 V. Uskoković and M. Drofenik, Reverse micelles: Inert nano-reactors or physico-chemically active guides of the capped reactions, *Adv. Colloid Interface Sci.*, 2007, **133**, 23–34.
13 M. A. López-Quintela, C. Tojo, M. C. Blanco, L. García Rio and J. R. Leis, Microemulsion dynamics and reactions in microemulsions, *Curr. Opin. Colloid Interface Sci.*, 2004, **9**, 264–278.
14 I. Capek, Preparation of metal nanoparticles in water-in-oil (w/o) microemulsions, *Adv. Colloid Interface Sci.*, 2004, **110**, 49–74.
15 K. Holmberg, Surfactant-templated nanomaterials synthesis, *J. Colloid Interface Sci.*, 2004, **274**, 355–364.
16 A. K. Ganguli, A. Ganguly and S. Vaidya, Microemulsion-based synthesis of nanocrystalline materials, *Chem. Soc. Rev.*, 2010, **39**, 474–485.
17 D. H. Chen and S. H. Wu, Synthesis of nickel nanoparticles in water-in-oil microemulsions, *Chem. Mater.*, 2000, **12**, 1354–1360.
18 J. Hernández, J. Solla-Gullón and E. Herrero, Gold nanoparticles synthesized in a water-in-oil microemulsion: electrochemical characterization and effect of the surface structure on the oxygen reduction reaction, *J. Electroanal. Chem.*, 2004, **574**, 185–196.
19 J. A. Gutierrez, J. J. Silber, R. D. Falcone and N. M. Correa, Modified reverse micelle method as facile way to obtain several gold nanoparticle morphologies, *J. Mol. Liq.*, 2021,

331, 115709.

20 D. Zhang, X. Liu, X. Wang, X. Yang and L. Lu, Optical properties of monodispersed silver nanoparticles produced via reverse micelle microemulsion, *Phys. B Condens. Matter*, 2011, **406**, 1389–1394.

21 O. P. Yadav, A. Palmqvist, N. Cruise and K. Holmberg, Synthesis of platinum nanoparticles in microemulsions and their catalytic activity for the oxidation of carbon monoxide, *Colloids Surfaces A Physicochem. Eng. Asp.*, 2003, **221**, 131–134.

22 M. Chen, Y. Feng, L. Wang, L. Zhang and J.-Y. Zhang, Study of palladium nanoparticles prepared from water-in-oil microemulsion, *Colloids Surfaces A Physicochem. Eng. Asp.*, 2006, **281**, 119–124.

23 B. Yoon, H. Kim and C. M. Wai, Dispersing palladium nanoparticles using a water-in-oil microemulsion—homogenization of heterogeneous catalysis, *Chem. Commun.*, 2003, **3**, 1040–1041.

24 S. Eriksson, Preparation of catalysts from microemulsions and their applications in heterogeneous catalysis, *Appl. Catal. A Gen.*, 2004, **265**, 207–219.

25 C. Liang, J. Han, K. Shen, L. Wang, D. Zhao and H. S. Freeman, Palladium nanoparticle microemulsions: Formation and use in catalytic hydrogenation of o-chloronitrobenzene, *Chem. Eng. J.*, 2010, **165**, 709–713.

26 A. Das, N. Yadav, S. Manchala, M. Bungla and A. K. Ganguli, Mechanistic Investigations of Growth of Anisotropic Nanostructures in Reverse Micelles, *ACS Omega*, 2021, **6**, 1007–1029.

27 M. A. López-Quintela, Synthesis of nanomaterials in microemulsions: Formation mechanisms and growth control, *Curr. Opin. Colloid Interface Sci.*, 2003, **8**, 137–144.

28 M. Chen, J. Falkner, W.-H. Guo, J.-Y. Zhang, C. Sayes and V. L. Colvin, Synthesis and self-organization of soluble monodisperse palladium nanoclusters, *J. Colloid Interface Sci.*, 2005, **287**, 146–151.

29 B. Richard, J.-L. Lemyre and A. M. Ritcey, Nanoparticle Size Control in Microemulsion Synthesis, *Langmuir*, 2017, **33**, 4748–4757.

30 A. M. Perez-Coronado, L. Calvo, N. Alonso-Morales, F. Heras, J. J. Rodriguez and M. A. Gilarranz, Multiple approaches to control and assess the size of Pd nanoparticles synthesized via water-in-oil microemulsion, *Colloids Surfaces A Physicochem. Eng. Asp.*, 2016, **497**, 28–34.

31 B. Sun, J. Chai, Z. Chai, X. Zhang, X. Cui and J. Lu, A surfactant-free microemulsion consisting of water, ethanol, and dichloromethane and its template effect for silica synthesis, *J. Colloid Interface Sci.*, 2018, **526**, 9–17.

32 S. Sharma, N. Yadav, P. K. Chowdhury and A. K. Ganguli, Controlling the Microstructure of Reverse Micelles and Their Templating Effect on Shaping Nanostructures, *J. Phys. Chem. B*, 2015, **119**, 11295–11306.

33 L. M. Magno, D. G. Angelescu, W. Sigle and C. Stubenrauch, Microemulsions as reaction media for the synthesis of Pt nanoparticles, *Phys. Chem. Chem. Phys.*, 2011, **13**, 3048–3058.

34 C. Tojo, D. Buceta and M. A. López-Quintela, Bimetallic nanoparticles synthesized in microemulsions: A computer simulation study on relationship between kinetics and metal segregation, *J. Colloid Interface Sci.*, 2018, **510**, 152–161.

35 M. Maillard, S. Giorgio and M.-P. Pileni, Tuning the Size of Silver Nanodisks with Similar Aspect Ratios: Synthesis and Optical Properties, *J. Phys. Chem. B*, 2003, **107**, 2466–2470.

36 M. A. López-Quintela, J. M. Rivas, C. Blanco, C. Tojo, M. Blanco and C. Tojo, in *Nanoscale Materials.*, eds. L. M. LM and K. PV, Kluwer Academic Publishing/Plenum, Boston, 2003, vol. 7028, pp. 135–155.

37 M. de Dios, F. Barroso, C. Tojo and M. A. López-Quintela, Simulation of the kinetics of nanoparticle formation in microemulsions, *J. Colloid Interface Sci.*, 2009, **333**, 741–748.

38 U. Natarajan, K. Handique, A. Mehra, J. R. Bellare and K. C. Khilar, Ultrafine Metal Particle Formation in Reverse Micellar Systems: Effects of Intermicellar Exchange on the Formation of Particles, *Langmuir*, 1996, **12**, 2670–2678.

39 R. P. Bagwe and K. C. Khilar, Effects of the Intermicellar Exchange Rate and Cations on the Size of Silver Chloride Nanoparticles Formed in Reverse Micelles of AOT, *Langmuir*, 1997, **13**, 6432–6438.

40 R. P. Bagwe and K. C. Khilar, Effects of intermicellar exchange rate on the formation of silver nanoparticles in reverse microemulsions of AOT, *Langmuir*, 2000, **16**, 905–910.

41 C. Tojo, M. C. Blanco and M. A. López-Quintela, Preparation of Nanoparticles in Microemulsions: A Monte Carlo Study of the Influence of the Synthesis Variables †, *Langmuir*, 1997, **13**, 4527–4534.

42 J. Eastoe, M. J. Hollamby and L. Hudson, Recent advances in nanoparticle synthesis with reversed micelles, *Adv. Colloid Interface Sci.*, 2006, **128–130**, 5–15.

43 H. H. Ingelsten, R. Bagwe, A. Palmqvist, M. Skoglundh, C. Svanberg, K. Holmberg and D. O. Shah, Kinetics of the Formation of Nano-Sized Platinum Particles in Water-in-Oil Microemulsions, *J. Colloid Interface Sci.*, 2001, **241**, 104–111.

44 S. De Marchi, S. Núñez-Sánchez, G. Bodelón, J. Pérez-Juste and I. Pastoriza-Santos, Pd nanoparticles as a plasmonic material: Synthesis, optical properties and applications, *Nanoscale*, 2020, **12**, 23424–23443.

45 C. F. Lo, K. Karan and B. R. Davis, Kinetic Studies of Reaction between Sodium Borohydride and Methanol, Water, and Their Mixtures, *Ind. Eng. Chem. Res.*, 2007, **46**, 5478–5484.

46 M. Wojnicki, K. Pacławski, E. Rudnik and K. Fitzner, Kinetics of palladium(II) chloride complex reduction in aqueous solutions using dimethylamineborane, *Hydrometallurgy*, 2011, **110**, 56–61.

47 M. Wojnicki, K. Fitzner and M. Luty-Błocho, Kinetic studies of nucleation and growth of palladium nanoparticles, *J. Colloid Interface Sci.*, 2016, **465**, 190–199.

48 D. Blach, N. M. Correa, J. J. Silber and R. D. Falcone, Interfacial water with special electron donor properties:

Effect of water-surfactant interaction in confined reversed micellar environments and its influence on the coordination chemistry of a copper complex, *J. Colloid Interface Sci.*, 2011, **355**, 124–130.

49 J. E. Martin, J. P. Wilcoxon, J. Odinek and P. Provencio, Superlattices of Platinum and Palladium Nanoparticles, *J. Phys. Chem. B*, 2002, **106**, 971–978.

50 L.-A. Nguyen Ly, R. G. Carbonell and B. J. Mc Coy, Diffusion of gases through surfactant films: Interfacial resistance to mass transfer, *AIChE J.*, 1979, **25**, 1015–1024.

51 K. E. Gubbins, K. K. Bhatia and R. D. Walker, Diffusion of gases in electrolytic solutions, *AIChE J.*, 1966, **12**, 548–552.

52 S. S. Atik and J. K. Thomas, Transport of photoproduced ions in water in oil microemulsions: movement of ions from one water pool to another, *J. Am. Chem. Soc.*, 1981, **103**, 3543–3550.

53 A. Jada, J. Lang, R. Zana, R. Makhloufi, E. Hirsch and S. J. Candau, Ternary water in oil microemulsions made of cationic surfactants, water, and aromatic solvents. 2. Droplet sizes and interactions and exchange of material between droplets, *J. Phys. Chem.*, 1990, **94**, 387–395.

54 P. D. I. Fletcherj, A. M. Howet, B. H. Robinson9, P. D. I. Fletcher, A. M. Howe, B. H. Robinson, P. D. I. Fletcherj, A. M. Howet and B. H. Robinson9, The Kinetics of Solubilisate Exchange between Water Droplets of a Water-in-oil Microemulsion, *J. Chem. SOC. Faraday Trans. I*, 1987, **83**, 985–1006.

55 H. Mays, J. Pochert and G. Ilgenfritz, Droplet Clustering in Ionic and Nonionic Water in Oil Microemulsion:: Rate of Exchange between Clusters Studied by Phosphorescence Quenching, *Langmuir*, 1995, **11**, 4347–4354.

56 H. friedrich Eicke, J. C. W. Shepherd and A. Steinemann, Exchange of solubilized water and aqueous electrolyte solutions between micelles in apolar media, *J. Colloid Interface Sci.*, 1976, **56**, 168–176.

57 A. Jada, J. Lang and R. Zana, Relation between electrical percolation and rate constant for exchange of material between droplets in water in oil microemulsions, *J. Phys. Chem.*, 1989, **93**, 10–12.

58 A. S. Bommarius, J. F. Holzwarth, D. I. C. Wang and T. A. Hatton, Coalescence and solubilizate exchange in a cationic four-component reversed micellar system, *J. Phys. Chem.*, 1990, **94**, 7232–7239.

59 N. T. K. Thanh, N. Maclean and S. Mahiddine, *Chem. Rev.*, 2014, 114, 7610–7630.

60 V. K. La Mer, Nucleation in Phase Transitions., *Ind. Eng. Chem.*, 1952, **44**, 1270–1277.

61 V. K. La Mer, R. H. Dinegar, V. K. Lamer and R. H. Dinegar, Theory, Production and Mechanism of Formation of Monodispersed Hydrosols, *J. Am. Chem. Soc.*, 1950, **72**, 4847–4854.

62 J. Lang, N. Lalem and R. Zana, Droplet size and dynamics in water-in-oil microemulsions, *Colloids and Surfaces*, 1992, **68**, 199–206.

63 H. Noritomi, N. Igari, K. Kagitani, Y. Umezawa, Y. Muratsubaki and S. Kato, Synthesis and size control of silver nanoparticles using reverse micelles of sucrose fatty acid esters, *Colloid Polym. Sci.*, 2010, **288**, 887–891.

64 H. Noritomi, Y. Umezawa, S. Miyagawa and S. Kato, Preparation of Highly Concentrated Silver Nanoparticles in Reverse Micelles of Sucrose Fatty Acid Esters through Solid-Liquid Extraction Method, *Adv. Chem. Eng. Sci.*, 2011, **01**, 299–304.